Molecular Conformation of Styrene on Ag(100): Relevance to an Understanding of the Catalytic Epoxidation of Terminal Alkenes

Federico J. Williams, Daniel P. C. Bird, E. Charles H. Sykes, Ashok K. Santra, and Richard M. Lambert*

Department of Chemistry, University of Cambridge, Cambridge CB2 1EW, England

Received: November 10, 2002

Fast XPS and NEXAFS have been used to investigate the adsorption, desorption, and molecular conformation of styrene adsorbed on Ag(100) in order to determine whether single-crystal studies on the catalytic oxidation of this molecule do indeed provide valid information relevant to a fundamental understanding of the Ag-catalyzed epoxidation of terminal alkenes, especially ethene. Styrene adsorbs and desorbs from the metal surface without decomposition and three states are discerned in the desorption spectra, depending on the coverage. The strongest and weakest bound states are associated with molecules in multilayer and submonolayer environments, respectively. XPS data indicate that a desorption peak that appears at intermediate coverages is associated with tilted molecules in the contact layer. In the coverage regime relevant to the catalytic epoxidation reaction, the phenyl and vinyl groups are coplanar, and the molecule lies flat on the metal surface. These observations validate the use of styrene as a model adsorbate with which to investigate the catalytic chemistry of terminal alkenes.

Introduction

Continued interest in the heterogeneously-catalyzed epoxidation of ethene derives both from the major technological importance of the industrial process and from the apparently unique behavior of silver as a catalyst−a fact that has stimulated much fundamental and applied research.[1] Single-crystal studies have played an important role in uncovering the long controversial molecular mechanism[2] and in elucidating the role of chlorine[3] and alkali promoters.[4] However, under ultrahigh vacuum conditions, measurements with ethene itself are not possible because the alkene adsorbs too weakly on Ag surfaces, even in the presence of oxygen. This limitation can be circumvented by making use of higher terminal alkenes which bind more strongly to clean silver surfaces, and the approach has been exploited by making use of the model alkenes norbornene,[5] 1-butene,[6] 2-methylpropene,[7] 3,3-dimethyl-1-butene,[8] butadiene,[9,10] and, especially, styrene (phenylethene).[11−14]

For example, studies of styrene epoxidation on Ag(111)[11] and Ag(100)[14] showed that the epoxidizing species was O(a) and that addition of Cl or K increased and decreased, respectively, the selectivity toward epoxide formation. Such results appear to validate the investigation of styrene epoxidation as a means of elucidating important aspects of ethene epoxidation. However, nothing is known about the orientation of styrene adsorbed on Ag, which raises significant issues when discussing the catalytic behavior of ethene in the light of styrene data. Ethene adsorbs with the crucially important C═C bond parallel to the metal surface.[15] On the other hand benzenoid species may adsorb in either flat[16] or tilted[17] geometries, and, in the case of styrene, there is the additional possibility of twisting about the C−C bond so that the phenyl and olefin functions are not coplanar. Thus, with adsorbed styrene a tilted phenyl group and/or twist about the C−C axis could result in the C═C function being located very differently with respect to the metal surface, compared to ethene. Indeed, on iron oxide single-crystal surfaces[18,19] and on Cu(110),[13] NEXAFS data show that styrene is substantially tilted at angles of 21°, and 39° (α-Fe_2O_3(0001) and FeO(111)) and 26° (Cu(110)), respectively. Thus, to have a complete microscopic picture of styrene epoxidation it is necessary to determine the orientation of styrene adsorbed on Ag under conditions that are relevant to the epoxidation reaction.

Here we present TPD, fast-XPS, and NEXAFS results which show that styrene adsorbs and desorbs reversibly from clean Ag(100) and that the adsorbed molecule is planar and lies parallel to the metal surface. These findings validate the use of styrene as a model terminal alkene for epoxidation studies on Ag, as there is no tilt or out-of-plane twisting of the olefin function that could endow it with significantly different reactive properties to those of ethene itself.

Experimental Methods

TPD Experiments. Temperature-programmed desorption (TPD) experiments were performed in Cambridge in a UHV chamber operated at a base pressure of 1×10^{-10} Torr; this apparatus, including methods of sample mounting, manipulation, and cleaning, has been described in detail elsewhere.[20] Reagent grade styrene was outgassed by means of 5 freeze−pump−thaw cycles and delivered to the sample via a tube doser; oxygen exposures were carried out by backfilling the vacuum chamber. TPD spectra were acquired at a heating rate of 5 K s^{-1}, while monitoring the relevant masses by means of a quadropole mass spectrometer whose ionizer was located ∼2 cm from the crystal face. With this geometry, essentially all the detected species arose from the front face of the sample.

F-XPS and NEXAFS Experiments. Fast X-ray photoelectron spectroscopy (F-XPS) and C K-edge NEXAFS measurements were carried out at the SuperESCA beamline at the ELETTRA synchrotron radiation facility in Trieste, Italy. The degree of linear polarization of the photons was 0.99 and photon

* Corresponding author. Tel: 44 1223 336467. Fax: 44 1223 336362. E-mail: RML1@cam.ac.uk.

10.1021/jp027422a CCC: $25.00
Published on Web 03/22/2003

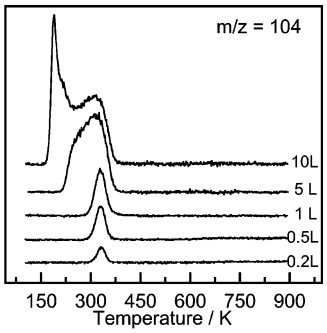

Figure 1. Styrene TPD data as a function of exposure at 100 K.

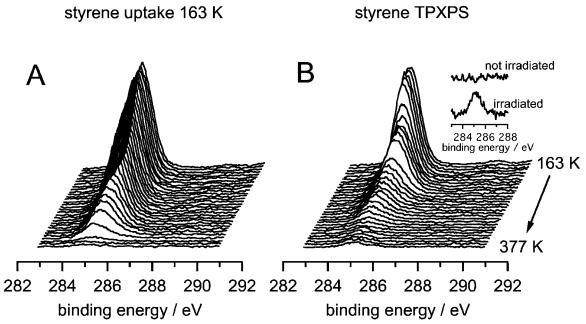

Figure 2. C 1s XP-spectra: (A) as a function of time during styrene uptake at 163 K; (B) temperature dependence during desorption of styrene.

energy was calibrated (±0.2 eV) by the position of the C−K edge dip in the monochromator output. XPS and NEXAFS spectra were collected with a double-pass 32-channel hemispherical electron analyzer, and the angle between the entrance lens of the analyzer and the incoming photon beam was 40° in the horizontal plane. Surface order and cleanliness were checked by LEED and XPS. Styrene uptakes were obtained by monitoring the C 1s XP spectra at constant temperature (150 K for multilayers and 220 K for a monolayer) while continuously dosing styrene at 5×10^{-10} Torr via a tube doser. Temperature-programmed XPS experiments (TP-XPS) were performed by dosing styrene at 150 K (multilayer) or 220 K (monolayer) and then ramping the temperature at 0.14 K s^{-1} while acquiring the C 1s XP spectra. The rate of XPS data acquisition was ∼30 s/spectrum. Quoted styrene coverages were determined by XPS with reference to the known[21] saturation coverage of atomic oxygen on Ag(100): 0.5 monolayers (ML) (1 ML is defined as the number of silver atoms in the first layer of the Ag(100) surface). Calibration was achieved by comparing the 0.5 ML O 1s intensity with that from the styrene adlayer due allowance being made for photoionization cross-sections and variations in photon flux.

Results and Discussion

Temperature-Programmed Desorption. Styrene adsorbed and desorbed reversibly; no other desorbing species were observed under any conditions, nor was carbon deposition detectable by Auger spectroscopy. Figure 1 shows styrene TPD spectra from the clean surface as a function of exposure at 100 K. For exposures in the range 0.2−1.0 L it is apparent that desorption was first-order with a peak at $T_p \sim 330$ K, close to the values reported for submonolayer styrene desorption from Ag(111) ($T_p \sim 330$ K[11]) and Ag(110) ($T_p \sim 370$ K[22]).

At 5 L exposure the broadened desorption peak exhibited a clear shoulder corresponding to a T_p of approximately 260 K which is due to styrene desorption from a new state. At 10 L exposure a sharp peak appeared at $T_p \sim 188$ K, which, by comparison with similar systems, may be assigned to multilayer desorption.[12,20] On the basis of first-order desorption we may use the method of Chan et al.[23,24] to estimate the zero-coverage kinetic constants. This procedure yields $E_d(\theta \rightarrow 0) = 71$ kJ/mol and $\nu(\theta \rightarrow 0) = 2 \times 10^{11}$ s^{-1} for desorption from the ∼330 K submonolayer state. Alternatively, following the simpler procedure proposed by Redhead[25] along with the above value for ν, one obtains values of ∼73 kJ/mol for the submonolayer state and ∼ 56 kJ/mol for the ∼260 K state.

Although the assignment of the ∼188 K and ∼330 K peaks is clear (multilayer and submonolayer desorption, respectively) assignment of the ∼ 260 K peak is less straightforward. Two possible explanations are (i) desorption from a second layer of molecules adorbed on top of the contact layer, or (ii) desorption of tilted molecules that are formed in the monolayer at sufficiently high coverages. In all reported cases where a second layer desorption peak has been observed, it occurs at 5−15 K above the multilayer peak,[26] very different from the present case. Consider on the other hand the case of benzene on Pd(111), where it is known that the monolayer contains only flat-lying molecules at low coverages with tilted molecules being formed in the contact layer at higher coverages. In that case the tilted molecule desorption peak is ∼130 K higher than the multilayer peak and ∼150 K lower than the flat-lying benzene peak.[27,28] Here, the ∼260 K peak lies 72 K higher than in the multilayer peak and 70 K lower than the submonolayer peak (we show below that this is associated with flat-lying styrene). Thus it seems likely that the ∼260 K peak corresponds to desorption from a relatively weakly bounded tilted configuration of styrene on the metal surface, a conclusion that receives support from the XPS results presented below.

Temperature-Programmed X-ray Photoelectron Spectroscopy. Figure 2A shows time-dependent C 1s spectra resulting from styrene uptake at 163 K, temperature at which multilayers are formed. A clear increase in the C 1s photoemission maximum with coverage is apparent. This increase in C 1s binding energy for the multilayer relative to the monolayer is likely due to a decrease in final state relaxation energy in the former case because the core hole is remote from the metal surface.

Once the multilayer signal had saturated (after 1100 s), the temperature was ramped from 163 to 377 K and C 1s spectra were acquired while styrene desorbed. The corresponding C 1s TP-XPS data are shown in Figure 2B. The final spectrum ($T =$ 377 K) shows a residual signal, presumably due to carbonaceous deposits; recall that the laboratory studies gave no evidence of styrene decomposition during desorption. Therefore, at the end of the TP-XPS experiment the X-ray beam was moved to a previously nonirradiated part of the sample and the corresponding C 1s XP spectra with and without irradiation are shown in the inset to Figure 2B. It is clear that a small degree of radiation-induced decomposition of styrene occurred over the course of these measurements.

The C 1s spectra shown in Figure 2 were fitted with a single Gaussian peak and the resulting integrated intensities presented in Figure 3. Styrene was admitted into the chamber ∼70 s after starting to acquire the spectra, as indicated by the arrow on the *x*-axis. Figure 3A shows the C 1s integrated intensity corresponding to the uptake results presented in Figure 2A. It is clear that after 900 s the C 1s signal saturated, indicating that the thickness of the multilayer film deposited on the Ag(100) surface exceeded the escape depth of the photoelectrons. Note the changes in slope at the points **x** and **y** which, by comparison with the TPD spectra, correspond to onset of the 260 K state and of multilayer occupancy, respectively. The linear segments

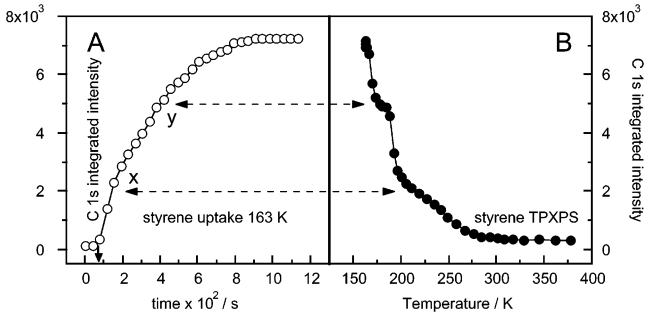

Figure 3. C 1s integrated intensities derived from the data in Figure 2.: (A) styrene uptake at 163 K, (B) styrene desorption.

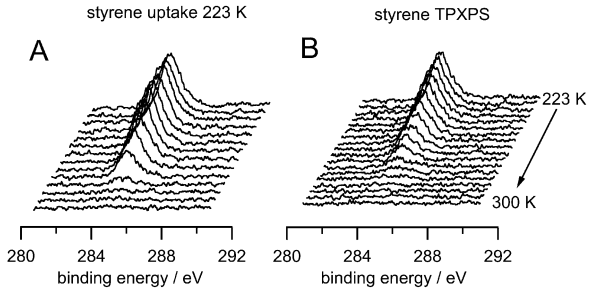

Figure 4. C 1s XP-spectra: (A) during uptake at 223 K, (B) during subsequent desorption.

imply approximately constant sticking probability into the 330 and 260 K states. Figure 3B shows the temperature dependence of the integrated C 1s intensity derived from Figure 2B. Note the breaks in the curve which correlate with **x**,**y** in Figure 3B. **y** corresponds to the termination of multilayer desorption (BE = 285.6 eV; fwhm ~ 1 eV; T_p = 188 K). **x** corresponds to the termination of desorption from the intermediate state (BE = 285.4 eV; fwhm ~ 1.3 eV; T_p = 260 K). The estimated saturation coverage of styrene in the high-temperature state is ~0.19 ML (styrene molecules/Ag surface atom); the total coverage when filling of the intermediate state (T_p = 260 K) is completed is ~0.48 ML. The ratio of these values is ~2.5, in good agreement with the value of ~2.6 estimated from the TPD peak areas.

Although we are not able to clearly resolve more than one peak in the XP spectra, the spectra corresponding to intermediate coverage (T_p ~ 260 K, BE = 285.4 eV, fwhm ~ 1.3 eV) are broadened to higher BE compared to those obtained at low coverage (T_p ~ 330 K, BE = 285.1 eV, fwhm ~ 1 eV). Therefore it is plausible to suppose that more than one species is present in the contact layer when the styrene coverage exceeds 0.19 ML. The NEXAFS results (below) show that the low-coverage state corresponds to a flat-lying molecule. Thus the 260 K state could correspond to tilted molecules, their geometry consistent with the reduced adsorption energy compared to the "flat" 330 K state. This is supported by the associated higher BE which lies between those characteristic of the flat and multilayer states. These results also indicate that appearance of the proposed tilted species does not result from a sharp flat-to-tilted phase transition at a particular coverage—since the two types of molecules coexist. This suggests that in the coverage regime 0.19 ML−0.48 ML the contact layer consists of a mixture of flat and tilted styrene molecules.

To characterize further the supposed "flat" state, styrene uptake was carried out at T = 223 K, where the saturation coverage of styrene is 0.19 ML (styrene molecules/surface Ag atom). Figure 4A shows the corresponding data. After saturation coverage was reached the temperature was ramped from 223 to 300 K and the resulting C 1s XP spectra are shown in Figure 4B. In this case no residual carbon was observed because (i) the total amount of styrene over the surface was much lower (submonolayer versus multilayer) and (ii) the exposure time to the synchrotron radiation was shorter.

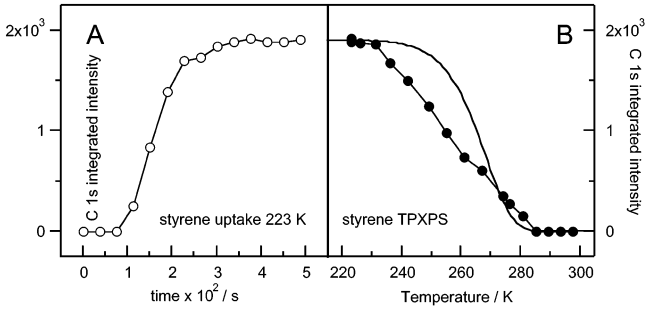

Figure 5. C 1s integrated intensities derived from the data shown in Figure 4: (A) uptake at 223 K, (B) subsequent temperature-programmed XPS; solid line (5B) shows the calculated coverage of styrene as a function of temperature.

Figure 5A,B shows the time and temperature dependence, respectively, of C 1s integrated intensities derived from Figure 4A,B. If we assume that the kinetic parameters are coverage-independent, the temperature dependence of the styrene coverage (θ) is given by

$$\frac{d\theta}{dT} = -\frac{\upsilon}{\beta} e^{-E/RT}\theta \qquad (1)$$

where β is the heating rate. Equation 1 can be integrated using the parameters estimated from the TPD results presented in Figure 1, i.e., E = 71 kJ/mol and $\nu = 2 \times 10^{11}$ s^{-1} with β = 0.14 K/s the heating rate used in the Trieste experiments. The solid line in Figure 5B shows the result along with the experimentally measured coverages (circles). It is clear that the agreement is satisfactory only at low coverages, indicating that the values for E and ν derived in the limit $\theta \rightarrow 0$ from the TPD data are good. The discrepancy apparent at higher coverages presumably reflects the effects of repulsive intermolecular interactions.

Near-Edge X-ray Adsorption Fine Structure Spectroscopy. Figure 6 shows adsorption step edge-normalized C K-edge NEXAFS spectra as a function of photon incident angle obtained after dosing the sample with 0.1 ML of styrene at 220 K. This is the coverage that is relevant to the catalytic epoxidation results obtained for styrene + O(a) on Ag(111)[11] and Ag(100).[14] (Due to lack of beam time, we were unable to take NEXAFS data at higher coverages). Normalization followed an established procedure involving division of the data by the clean surface NEXAFS spectrum.[29] In Figure 6 the experimental data are represented by the heavy solid line and the individual fitted components are represented by thin lines. The top panel shows a magnified portion of the 10° spectrum to make clearer the presence of two components within the envelope of the leading peak. The overall envelope can be fitted with two Gaussians *A*, *A*′, with same half width and with intensity ratio 3:1. The relative positions of these two components are in good accord with the π^* resonances of adsorbed benzene[30] and ethene.[31] Moreover, both resonances have been observed in the NEXAFS spectrum of styrene, whereas only the high photon energy component is seen in the NEXAFS spectrum of both benzene and ethylbenzene.[18,19] Therefore we assign *A* and *A*′ to π^* resonances associated with the phenyl and vinyl functions of styrene, respectively. A third π^* resonance labeled *C* is also apparent. Features *D* and *E* are σ^* resonances and not of interest with

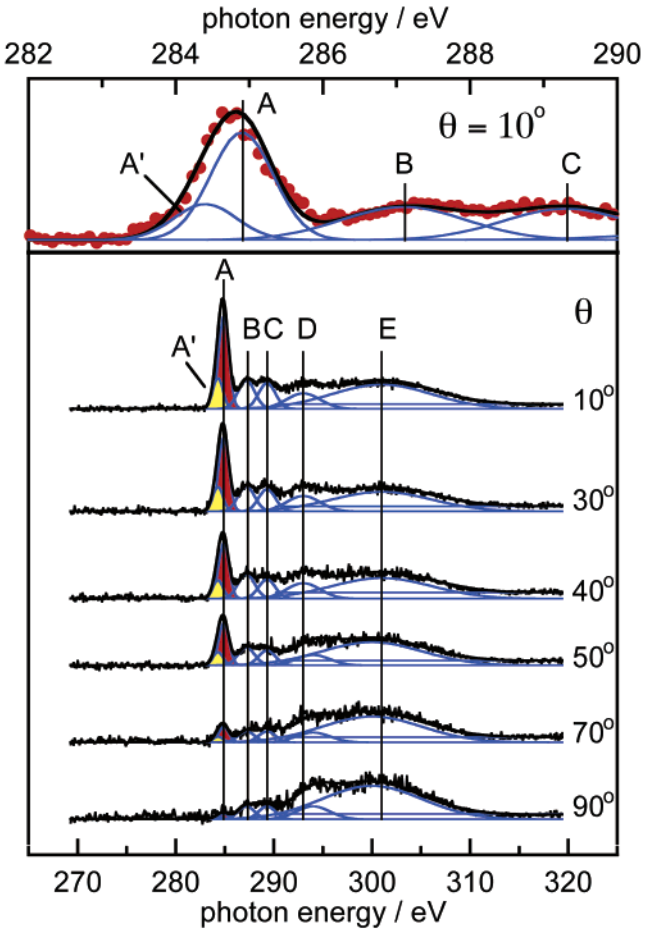

Figure 6. C 1s NEXAFS spectra taken from 0.1 ML of styrene adsorbed at 220 K as a function of photon incidence angle. Top panel shows magnification of leading feature and resolution into components A and A′.

TABLE 1: Observed Energies and Assignments of NEXAFS Resonances Shown in Figure 6

resonance	energetic position (eV)	assigment
A′	284.3	C 1s → π^* (vinyl group)
A	285	C 1s → π^* (phenyl group)
B	287	Rydberg
C	289	C 1s → π^* (phenyl group)
D	293	C 1s → σ^*
E	301	C 1s → σ^*

respect to the determination of adsorption geometry. Table 1 summarizes peak positions and assignments, the latter being obtained from the results of Whün[18] and of Joseph et al.[19] The edge jump is shown as a solid line and was set at the XPS binding energy plus the work function of the clean surface (4.64 eV[32]).

The electronic excitation from the C 1s level into the unoccupied orbitals π^* and σ^* depend on the molecular orientation with respect to the electric field vector of the polarized radiation. For a planar aromatic molecule (such as styrene in the gas phase), the C 1s → π^* transition is polarized perpendicular to the molecular plane and therefore the dipole selection rules require this transition to be excited by the component of the electric field perpendicular to the molecular plane. Thus, the C 1s → π^* transition has maximum (zero) intensity when the electric field vector is oriented perpendicular (parallel) to the molecular plane. On the contrary, the C 1s → σ^* transition is polarized parallel to the molecular plane and then it has maximum (zero) intensity when the electric field

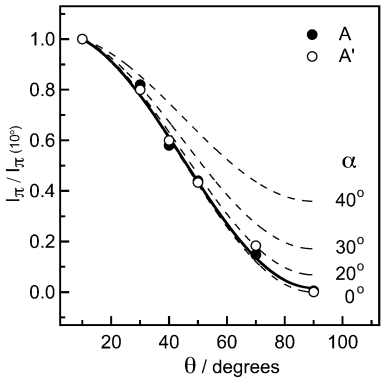

Figure 7. A, A′ resonance intensities normalized to the intensity at 10°. Best fit corresponds to an apparent tilt angle of 5°.

vector is oriented parallel (perpendicular) to the molecular plane. Hence, if the molecule is adsorbed with its molecular plane parallel to the surface then the C 1s → π^* (C 1s → σ^*) transition has maximum (minimal) intensity at grazing incidence and minimal (maximum) intensity at normal incidence. The spectra presented in Figure 6 show that with increasing photon incidence angle from 10° (grazing incidence) to 90° (normal incidence) all π^* intensities decrease and the opposite trend is observed for the σ^* resonances. Therefore, the above indicates at least qualitatively that adsorbed styrene on Ag(100) is oriented with its molecular plane parallel to the surface.

A quantitative estimation of the angle (α) between the unoccupied vector orbital under study and the surface normal can be obtained from the polarization dependence of C 1s → π^* intensities, following well-established procedures. For surfaces with 3-fold symmetry or higher, this dependence is given by[33]

$$I_\pi(\theta,\alpha) \sim P(\sin^2\alpha \sin^2\theta + 2\cos^2\alpha \cos^2\theta) + (1-P)\sin^2\alpha \quad (2)$$

where θ is the photon incidence angle and P is the degree of linear polarization of the synchrotron radiation. Figure 7 shows the measured angular dependence of intensity for resonances *A* and *A′* along with $I_\pi(\theta,\alpha)$ curves for a range of α values, calculated according to eq 2. The best fit yields an apparent tilt angle of 5° ± 5° for both the *A* and *A′* data. The implications are that (i) the phenyl and vinyl groups are coplanar, and (ii) the molecule lies essentially flat on the metal surface. This final observation validates the use of styrene as a model terminal alkene for epoxidation studies as there is no out-of-plane twisting of the vinyl function that could endow it significantly different reactive properties. Related to this, it is interesting to note that on clean Cu(110) the epoxidation of tilted styrene proceeds with ∼100% selectivity, whereas on clean Ag{100} the selectivity is only ∼50% with substantial amounts of CO_2 and H_2O formed along with the epoxide.[14] It is tempting to speculate that, on Cu(110), tilting the vinyl function away from the surface renders it immune to H-abstraction and eventual combustion, whereas these processes clearly can occur for flat styrene on Ag(100).

Conclusions

1. Styrene adsorbs and desorbs from a Ag(100) surface without decomposition. Three states are discernible in the desorption spectra, depending on the coverage. The strongest and weakest bound states are associated with molecules in multilayer and submonolayer environments, respectively. An intermediate desorption peak that appears at coverages >∼0.19

ML (styrene molecules/Ag surface atom) is likely due to tilted molecules in the contact layer.

2. The activation energy and preexponential factor for desorption in the limit $\theta \rightarrow 0$ for the submonolayer state (0−0.19 ML) are $E \sim 71$ kJ/mol and $\nu \sim 2 \times 10^{11}$ s^{-1}, respectively. TPXPS results suggest that styrene−styrene intermolecular repulsions cannot be neglected at high styrene coverage.

3. In the coverage regime relevant to the Ag-catalyzed catalytic epoxidation of styrene, the phenyl and vinyl groups are parallel, and the molecule lies flat on the metal surface.

4. These observations validate the use of styrene as a model adsorbate with which to investigate the catalytic chemistry of terminal alkenes, and especially ethene itself.

Acknowledgment. Financial support from the UK Engineering and Physical Sciences Research Council under Research Grant GR/M76706 is gratefully acknowledged. F.J.W. acknowledges the award of a Cambridge University Oppenheimer Fellowship.

References and Notes

(1) Serafin, J. G.; Liu, A. C.; Seyedmonir, S. R. *J. Mol. Catal. A* **1998**, *131*, 157−168.
(2) Grant, R. B.; Lambert, R. M. *J. Catal.* **1985**, *92*, 364−375.
(3) Tan, S. A.; Grant, R. B.; Lambert, R. M. *J. Catal.* **1986**, *100*, 383−391.
(4) Grant, R. B.; Lambert, R. M. *J. Catal.* **1985**, *93*, 92−99.
(5) Roberts, J. T.; Madix, R. J. *J. Am. Chem. Soc.* **1988**, *110*, 8540−8541.
(6) Roberts, J. T.; Capote, A. J.; Madix, R. J. *Surf. Sci.* **1991**, *253*, 13−23.
(7) Ayre, C. R.; Madix, R. J. *Surf. Sci.* **1992**, *262*, 51−67.
(8) Mukoid, C.; Hawker, S.; Badyal, J. P. S.; Lambert, R. M. *Catal. Lett.* **1990**, *4*, 57−61.
(9) Roberts, J. T.; Capote, A. J.; Madix, R. J. *J. Am. Chem. Soc.* **1991**, *113*, 9848−9851.
(10) Cowell, J. J.; Santra, A. K.; Lambert, R. M. *J. Am. Chem. Soc.* **2000**, *122*, 2381−2382.
(11) Hawker, S.; Mukoid, C.; Badyal, J. P. S.; Lambert, R. M. *Surf. Sci.* **1989**, *219*, L615−L622.
(12) Santra, A. K.; Cowell, J. J.; Lambert, R. M. *Catal. Lett.* **2000**, *67*, 87−91.
(13) Cowell, J. J.; Santra, A. K.; Lindsay, R.; Lambert, R. M.; Baraldi, A.; Goldoni, A. *Surf. Sci.* **1999**, *437*, 1−8.
(14) Williams, F. J.; Bird, D. P. C.; Santra, A. K.; Sykes, E. C. H.; Lambert, R. M. In preparation.
(15) Arvanitis, D.; Baberschke, K.; Wenzel, L.; Dobler, U. *Phys. Rev. Lett.* **1986**, *57*, 3175−3178.
(16) Netzer, F. P. *Langmuir* **1991**, *7*, 2544−2547.
(17) Yannoulis, P.; Dudde, R.; Frank, K. H.; Koch, E. E. *Surf. Sci.* **1987**, *189*, 519−528.
(18) Wühn, M.; Joseph, Y.; Bagus, P. S.; Niklewski, A.; Püttner, R.; Reiss, S.; Weiss, W.; Martins, M.; Kaindl, G.; Wöll, C. *J. Phys. Chem. B* **2000**, *104*, 7694−7701.
(19) Joseph, Y.; Wühn, M.; Niklewski, A.; Ranke, W.; Weiss, W.; Wöll, C.; Schlögl, R. *Phys. Chem. Chem. Phys.* **2000**, *2*, 5314−5319.
(20) Wilson, K.; Lee, A. F.; Hardacre, C.; Lambert, R. M. *J. Phys. Chem. B* **1998**, *102*, 1736−1744.
(21) Fang, C. S. A. *Surf. Sci.* **1990**, *235*, L291−L294.
(22) Carlo, S. R.; Grassian, V. H. *Langmuir* **1997**, *13*, 2307−2313.
(23) Chan, C. M.; Aris, R.; Weinberg, W. H. *Appl. Surf. Sci. 1978*, *1*, 360−376.
(24) Jong, A. M.; Niemantsverdriet, J. W. *Surf. Sci.* **1990**, *233*, 355−365.
(25) Redhead, P. A. *Vacuum* **1962**, *12*, 203−211.
(26) Xi, M.; Yang, M. X.; Jo, S. K.; Bent, B. E.; Stevens, P. *J. Chem. Phys.* **1994**, *101*, 9122−9130.
(27) Hoffmann, H.; Zaera, F.; Ormerod, R. M.; Lambert, R. M.; Wang, L. P.; Tysoe, W. T. *Surf. Sci.* **1990**, *232*, 259−265.
(28) Lee, A. F.; Wilson, K.; Lambert, R. M.; Goldoni, A.; Baraldi, A.; Paolucci, G. *J. Phys. Chem. B* **2000**, *104*, 11729−11733.
(29) Outka, D. A.; Stöhr, J. *J. Chem. Phys.* **1988**, *88*, 3539−3553.
(30) Solomon, J. L.; Madix, R. J.; Sthör, J. *Surf. Sci.* **1991**, *255*, 12−30.
(31) Rabus, H.; Arvanitis, D.; Baberschke, K. *Surf. Sci.* **1992**, *269/270*, 270−275.
(32) Skriver, H. L.; Rosengaard, N. M. *Phys. Rev. B* **1992**, *46*, 7157−7168.
(33) Ernst, K. H.; Neuber, M.; Grunze, M.; Ellerbeck, U. *J. Am. Chem. Soc.* **2001**, *123*, 493−495.